

Deep Reinforcement Learning Optimization for Uncertain Nonlinear Systems via Event-Triggered Robust Adaptive Dynamic Programming

Ningwei Bai * Chi Pui Chan * Qichen Yin * Tengyang Gong **
Yunda Yan * Zehzi Tang *

* Department of Computer Science, University College London, Gower Street, London, WC1E 6BT United Kingdom (e-mail: zehzi.tang@ucl.ac.uk).

** Department of Electrical and Electronic Engineering, University of Manchester, Oxford Rd, Manchester, M13 9PL United Kingdom

Abstract: This work proposes a unified control architecture that couples a Reinforcement Learning (RL)-driven controller with a disturbance-rejection Extended State Observer (ESO), complemented by an Event-Triggered Mechanism (ETM) to limit unnecessary computations. The ESO is utilized to estimate the system states and the lumped disturbance in real time, forming the foundation for effective disturbance compensation. To obtain near-optimal behavior without an accurate system description, a value-iteration-based Adaptive Dynamic Programming (ADP) method is adopted for policy approximation. The inclusion of the ETM ensures that parameter updates of the learning module are executed only when the state deviation surpasses a predefined bound, thereby preventing excessive learning activity and substantially reducing computational load. A Lyapunov-oriented analysis is used to characterize the stability properties of the resulting closed-loop system. Numerical experiments further confirm that the developed approach maintains strong control performance and disturbance tolerance, while achieving a significant reduction in sampling and processing effort compared with standard time-triggered ADP schemes.

Keywords: Reinforcement learning; Event-triggered control; Uncertain nonlinear systems; Adaptive dynamic programming

1. INTRODUCTION

Learning-based methods have become a fundamental paradigm in modern engineering systems, enabling algorithms to improve performance through data-driven adaptation without relying solely on explicit mathematical models. Over the past decade, advances in machine learning, particularly in function approximation, optimization, and representation learning, have significantly expanded the capability of intelligent systems operating under uncertainty, compared to traditional analytical methods (Qin et al. (2023); Zhang et al. (2024); Hu et al. (2025)). These approaches have been increasingly adopted in control, robotics, and even generative language models (Lu et al. (2020); Zhao et al. (2024); Tang et al. (2025); Yao et al. (2025)). However, conventional model-based techniques may be limited in their ability to handle nonlinearities, unknown disturbances, or incomplete system knowledge.

Reinforcement Learning (RL) has gained attention for complex decision-making and control in uncertain, dynamic environments (Tang et al. (2024d)). In control engineering, RL-based methods offer a data-driven alternative to classical model-based designs. This is useful when accurate system models are difficult to obtain. Among

these methods, ADP integrates RL with optimal control theory. It facilitates near-optimal control of nonlinear systems by approximating value functions and control policies through function approximators. This eliminates the need to explicitly solve the Hamilton–Jacobi–Bellman (HJB) equation (Lewis and Vrabie (2009)). However, conventional ADP frameworks often rely on continuous or periodic updates to neural network parameters. These updates impose significant computational burdens and may lead to overfitting to transient disturbances or noise.

Event-triggered strategies have been widely adopted in diverse control applications, including networked and embedded systems, multi-agent coordination, and resource-constrained robotic platforms (Onuoha et al. (2024b,a)). Meanwhile, the ETM has been widely employed in both control and ADP frameworks to reduce computational load (Han et al. (2024); Heemels et al. (2012); Tabuada (2007)). Unlike time-driven schemes, ETMs update only when systems meet a state- or error-based condition. State deviation or estimation error often directly triggers updates. This approach reduces redundant updates and preserves closed-loop stability (Dong et al. (2017); Xue et al. (2020); Onuoha et al. (2024b)). By limiting updates

to key events, event-triggered ADP boosts efficiency and yields policies less sensitive to disturbances.

Despite these advantages, engineers must ensure robustness against external disturbances and modeling uncertainties. In practice, environmental perturbations, unmodeled dynamics, nonlinear couplings, and parameter uncertainties cause disturbances. Many robust control approaches employ feedback to reduce perturbations rather than explicitly use feedforward compensation (Tang (2019); Tang et al. (2016, 2024a)). In this context, a ESO estimates the original states and accumulated interference in real time. This allows proactive compensation of parameter mismatches, unmodeled dynamics, and external perturbations in nonlinear systems (Luo et al. (2020); Tang et al. (2024c); Han (2009); Chen et al. (2016); Ran et al. (2021); Pu et al. (2015); Tang et al. (2019)).

Recent work combines ESO-based disturbance rejection with RL for uncertain nonlinear systems (Ran et al. (2022); Tang et al. (2024b)). However, these ESO-RL schemes primarily operate in a time-driven manner: both the controller and learning updates run continuously or periodically, lacking an event-triggered learning mechanism. Many continuous-time ADP designs also impose restrictive Persistence of Excitation (PE) conditions for parameter convergence (Kamalapurkar et al. (2016)), making them hard to verify and enforce in practice.

Inspired by these observations, we develop a composite control framework for output-feedback control of uncertain nonlinear systems with lumped disturbances. The main contributions are summarized as follows:

- (1) A unified control structure incorporating ETM is developed, in which ESO-based state estimation, disturbance compensation, and controller updates occur only at triggering instants. The resulting unified composite control framework enables an aperiodic and computationally efficient realization of output-feedback RL control. By integrating ESO-based disturbance rejection with event-triggered RL, this work establishes a unified architecture not addressed in existing literature.
- (2) We propose an event-triggered learning rule for a simulation-of-experience ADP scheme, where critic and actor networks are updated solely at triggering instants using both instantaneous and Extrapolated Bellman Error (EBE). In contrast to existing ESO-RL frameworks (Ran et al. (2022); Tang et al. (2024b)), which employ continuous or periodic learning, the proposed mechanism produces an aperiodic, data-efficient adaptation. The associated analysis shows that practical stability and Uniform Ultimate Boundedness (UUB) are achieved without imposing a classical PE condition (Kamalapurkar et al. (2016)), while avoiding redundant high-frequency learning updates.

The remainder of the paper is structured as follows: Section II presents the problem and the system model. Section III describes the proposed composite control framework. Section IV describes the overall composite control framework. The simulation results are demonstrated in Section

V, and Section VI summarizes this paper and outlines potential directions for future research.

2. PROBLEM FORMULATION

In this paper, we identify the control of a set of uncertain affine nonlinear systems described by

$$\begin{cases} \dot{z} = f_z(x, z, \eta), \\ \dot{x} = Ax + B[f(x, z, \eta) + g(x, z, \eta)u], \\ y = Cx, \end{cases} \quad (1)$$

where $x = [x_1, \dots, x_n]^T \in \mathbb{R}^n$ denotes the state of the measured subsystem with relative degree n ; $z \in \mathbb{R}^p$ represents the zero-dynamics state; $\eta \in \mathbb{R}$ denotes an external disturbance or uncertain parameter; $u \in \mathbb{R}$ is the control input; $f_z : \mathbb{R}^n \times \mathbb{R}^p \times \mathbb{R} \rightarrow \mathbb{R}^p$ is a smooth nonlinear mapping describing the evolution of zero dynamics; $f, g : \mathbb{R}^n \times \mathbb{R}^p \times \mathbb{R} \rightarrow \mathbb{R}$ are uncertain nonlinear functions characterizing the input and drift dynamics gain of the x subsystem; and $A \in \mathbb{R}^{n \times n}$, $B \in \mathbb{R}^{n \times 1}$ and $C \in \mathbb{R}^{1 \times n}$ are the standard companion matrices defining a nominal chain-of-integrators structure of the output dynamics.

To enable subsequent observer and controller design, we impose the following standard assumptions.

Assumption 1. *The external signal $\eta(t)$ as well as its time derivative $\dot{\eta}(t)$ are bounded for all $t \geq 0$.*

Assumption 2. *The zero dynamics $\dot{z} = f_z(x, z, \eta)$ with input (x, η) is Bounded-Input Bounded-State (BIBS) stable.*

In this paper, the nonlinear system dynamics with uncertainty are modeled as follows:

$$\begin{aligned} f(x, z, \eta) &= f_0(x) + \Delta f(x, z, \eta), \\ g(x, z, \eta) &= g_0(x) + \Delta g(x, z, \eta), \end{aligned}$$

where $f_0, g_0 : \mathbb{R}^n \rightarrow \mathbb{R}$ denote the known nominal system dynamics; and $\Delta f, \Delta g : \mathbb{R}^n \times \mathbb{R}^p \times \mathbb{R} \rightarrow \mathbb{R}$ represent unknown disturbances and model uncertainties that may depend on the full state of the system (x, z) and the external signal η .

Following the Active Disturbance Rejection Control (ADRC) philosophy (Han (2009)), the general uncertainty is transferred to a broader state:

$$x_{n+1} \triangleq \Delta f(x, z, \eta) + \Delta g(x, z, \eta)u, \quad (2)$$

According to this definition, the n -th subsystem dynamics can be rewritten as $\dot{x}_n = x_{n+1} + f_0(x) + g_0(x)u$, so that the overall system becomes an $(n+1)$ th order augmented integrator chain perturbed by the unknown term \dot{x}_{n+1} .

To quantify performance, we consider the nominal compensated subsystem and assign the infinite-horizon cost functional

$$J(x_0) = \int_0^\infty (Q(x(\tau)) + u_0(\tau)^T R u_0(\tau)) d\tau, \quad (3)$$

where $x_0 = x(0)$ is the initial condition, $Q : \mathbb{R}^n \rightarrow \mathbb{R}_+$ is a positive definite state penalty, $R > 0$ is a control-weighting matrix, and u_0 denotes the component of the input acting on the nominal dynamics after uncertainty compensation.

The associated optimal control problem is

$$u_0^* = \arg \min_{u_0} J(x_0),$$

and the optimal policy will be approximated online via the RL mechanism developed later.

Remark 1. The purpose of this paper is to develop a ESO-based RL disturbance rejection scheme equipped with an ETM. The proposed controller aims to stabilize the system under lumped uncertainties while achieving near-optimal performance with reduced control update frequency.

3. COMPOSITE CONTROL FRAMEWORK

3.1 ESO Design

First, a ESO is designed to predict both the state of the system and all disturbances, following the standard ADRC structure (Han (2009); Chen et al. (2016)):

$$\begin{cases} \dot{\hat{x}}_i = \hat{x}_{i+1} + \frac{l_i}{\epsilon^i} (y - \hat{x}_1) & i = 1, \dots, n-1, \\ \dot{\hat{x}}_n = \hat{x}_{n+1} + \frac{l_n}{\epsilon^n} (y - \hat{x}_1) + f_0(\hat{x}) + g_0(\hat{x})u, \\ \dot{\hat{x}}_{n+1} = \frac{l_{n+1}}{\epsilon^{n+1}} (y - \hat{x}_1), \end{cases} \quad (4)$$

where $\hat{x} = [\hat{x}_1, \dots, \hat{x}_n, \hat{x}_{n+1}]^T$, $\epsilon > 0$ is a small positive constant adjusting the observer bandwidth, and $L = [l_1, \dots, l_{n+1}]^T$ is chosen that the following matrix is Hurwitz:

$$E = \begin{bmatrix} -l_1 & 1 & 0 & \cdots & 0 \\ -l_2 & 0 & 1 & \cdots & 0 \\ \vdots & \vdots & \vdots & \ddots & \vdots \\ -l_n & 0 & 0 & \cdots & 1 \\ -l_{n+1} & 0 & 0 & \cdots & 0 \end{bmatrix} \in \mathbb{R}^{(n+1) \times (n+1)}.$$

However, since the observer gains are scaled by ϵ^{-i} , a small ϵ yields a high bandwidth ESO that responds rapidly to state deviations but may induce a pronounced peaking phenomenon during the initial transient. To mitigate this effect, we employ a widely used smooth saturation technique to constrain the observer outputs. Let the saturated observer states be defined as

$$\bar{x}_i = M_i s\left(\frac{\hat{x}_i}{M_i}\right), \quad i = 1, \dots, n+1,$$

where $M_i > 0$ are design bounds selected so that the saturation remains inactive during steady-state operation, and $s(\cdot)$ is an odd, continuously differentiable saturation-like function given by

$$s(v) = \begin{cases} v, & 0 \leq v \leq 1 \\ v + \frac{v-1}{\varepsilon} - \frac{v^2-1}{2\varepsilon}, & 1 \leq v \leq 1 + \varepsilon \\ 1 + \frac{\varepsilon}{2}, & v > 1 + \varepsilon, \end{cases}$$

which satisfies $0 \leq s'(v) \leq 1$, $|s(v) - \text{sat}(v)| \leq \frac{\varepsilon}{2}$, $\forall v \in \mathbb{R}$. For later use, we denote $\bar{x} = [\bar{x}_1, \dots, \bar{x}_{n+1}]^T \in \mathbb{R}^{n+1}$ and observe that $\dot{\bar{x}}_i = s'\left(\frac{\hat{x}_i}{M_i}\right) \dot{\hat{x}}_i$, $i = 1, \dots, n+1$.

3.2 ADP Design

Second, we present the ADP design. An actor-critic architecture that is based on a neural network is employed, in which the critic approximates the optimal value function and the actor represents the corresponding optimal policy.

To facilitate the theoretical development of the ADP-based controller and the associated optimized control law, the following standard assumptions are introduced:

Assumption 3. There exist constants $g_{\min}, g_{\max} > 0$ such that

$$g_{\min} \leq \inf_{x \in \mathcal{X}} |g_0(x)| \leq \sup_{x \in \mathcal{X}} |g_0(x)| \leq g_{\max}.$$

Moreover, on $\Omega \triangleq \mathcal{X} \times \mathcal{Z} \times \mathcal{W}$ (where \mathcal{W} is a compact set containing all admissible values of η from Assumption 2, \mathcal{X} is a compact set containing all admissible system states x , and \mathcal{Z} is a bounded positively invariant set for the zero-dynamics state z), the relative mismatch between the true and nominal input gains is bounded

$$\kappa_g \triangleq \sup_{(x, z, \eta) \in \Omega} \frac{|g(x, z, \eta) - g_0(x)|}{|g_0(x)|} < 1.$$

As shown in (3), the associated value equation can be derived as follows

$$V(x) = \min_u J(x) = \int_0^\infty (Q(x(\tau)) + u(\tau)^T R u(\tau)) d\tau.$$

The optimal value equation $V(x)$ satisfies the HJB equation

$$0 = \min_u [Q(x) + u^T R u + \nabla V(x)^T (f(x, z, \eta) + g(x, z, \eta)u)].$$

gives the corresponding optimized control law

$$u^*(x) = -\frac{1}{2} R^{-1} g(x, z, \eta)^T \nabla V(x). \quad (5)$$

Substituting (5) into the HJB yields

$$\begin{aligned} 0 &= Q(x) + \nabla V(x)^T f(x, z, \eta) \\ &\quad - \frac{1}{4} \nabla V(x)^T g(x, z, \eta) R^{-1} g(x, z, \eta)^T \nabla V(x). \end{aligned}$$

This expression provides the optimality condition for the value equation and forms the basis for the subsequent critic approximation in the ADP framework.

3.3 Training Process

To avoid explicitly solving the HJB equation, we adopt an actor-critic architecture enhanced with an ESO-based extrapolation mechanism (Ran et al. (2022)). The critic network approximates the value function using a linearly parameterized structure.

$$V(\bar{x}; W_c) = W_c^T \phi(\bar{x}),$$

where W_c denotes the critic weight vector and $\phi(x)$ represents a basis vector.

The actor approximates the control policy as

$$u_0(\bar{x}; W_a) = -\frac{1}{2} R^{-1} g_0(\bar{x}) B^T \phi_x^T(\bar{x}) W_a,$$

where W_a is the actor weight vector and ϕ_x is the gradient of the basis function vector

Using the ESO-estimated state \hat{x} , the Instantaneous Bellman Error (IBE) is defined as

$$\begin{aligned} \varepsilon_t &\triangleq V_x(\bar{x}, W_a) \left[A\bar{x} + B(f_0(\bar{x}) + g_0(\bar{x})u_0(\bar{x}, W_a)) \right] \\ &\quad + Q(\bar{x}) + u_0^T(\bar{x}, W_c) R u_0(\bar{x}, W_c), \end{aligned} \quad (6)$$

which measures the deviation of the current actor-critic pair from the HJB optimality condition along the real trajectory.

To enhance state-space coverage and improve robustness, an extrapolated dataset $\mathcal{X}_E = \{\xi^i\}_{i=1}^N$ is generated in the

Algorithm 1 Composite Control Framework

- 1: **Initialization**
- 2: Set critic and actor weights $W_c(0)$ and $W_a(0)$
- 3: Initialize ESO states $z(0)$ in (4)
- 4: Set initial triggering instant $\tau_0 = 0$ and store $x(\tau_0)$ and $u(\tau_0)$
- 5: Generate extrapolation set \mathcal{X}_E for computing EBE
- 6:
- 7: Online Control Loop
- 8: At each time t :
- 9: Update ESO via (4) to obtain $\hat{x}(t)$ and $\hat{x}_{n+1}(t)$
- 10: Compute triggering error using (3.4)
- 11: Evaluate threshold $\delta(t)$ via (3.4)
- 12: Check triggering condition (3.4)
- 13: If the triggering condition is satisfied then
- 14: Compute IBE ε_t using (6).
- 15: Compute EBE ε_i using (7)
- 16: Update critic weights W_v via (8)
- 17: Update actor weights W_a via (9)
- 18: Compute new control input u using (3.3)
- 19: Set $\tau_{k+1} = t$ and store $\hat{x}(\tau_{k+1})$ and $u(\tau_{k+1})$
- 20: Else
- 21: Hold $u(t) = u(\tau_k)$ via ZOH.
- 22: End if
- 23: Apply $u(t)$ to the plant dynamics (1).

asymptotically stable; (iii) the uncertainty compensation renders the plant dynamics equivalent to the nominal model used in the ADP design; and (iv) the estimation errors of the actor-critic neural-network weights are uniformly ultimately bounded. Then all closed-loop signals are uniformly ultimately bounded, and the state $x(t)$ converges to a small neighborhood of the origin.

Proof. We provide a sketch of the argument. Consider the Lyapunov candidate

$$V = V^*(x) + \frac{1}{2}(\Theta_v^e)^T \Gamma^{-1} \Theta_v^e + \frac{1}{2}(\Theta_c^e)^T \Theta_c^e.$$

where $V^*(x)$ is the optimal value function, and Θ_v^e, Θ_c^e denote the critic and actor weight errors, respectively.

On each inter-event interval $[\tau_k, \tau_{k+1})$, the ESO, the control policy, and the actor-critic weights are fixed. Under the proposed control law, standard Lyapunov analysis yields

$$\dot{V} \leq -\alpha \|x\|^2 + \mathcal{O}(\varepsilon),$$

for some $\alpha > 0$ and sufficiently small approximation and estimation errors, implying boundedness of all closed-loop variables on each inter-event interval. At each triggering instant, the ESO correction and the actor-critic updates are designed so that V does not increase, which ensures UUB of $(x, \Theta_v^e, \Theta_c^e)$.

By Assumption 1, the inter-event times satisfy $\tau_{k+1} - \tau_k \geq \tau_{\min} > 0$, which excludes Zeno behavior and guarantees that only finitely many events occur on any finite time interval.

Combining these properties shows that this composite control framework system is uniformly ultimately bounded and that $x(t)$ converges to a small neighborhood of the origin. \square

Remark 2. The above Lyapunov analysis is carried out only on the continuous-time closed loop between triggering instants. The event-triggering error $e(t)$ is not explicitly included in the Lyapunov function. As a result, the analysis provides practical stability within each inter-event interval, but does not constitute a full hybrid-system proof. A rigorous global stability proof would require augmenting the Lyapunov function with $e(t)$ and deriving an ISS-type inequality of the form

$$\dot{V} \leq -k_1 \|x\|^2 + k_2 \|e\|^2, \quad (6)$$

where $k_1 > 0$ is the nominal decay rate of the Lyapunov function, $k_2 > 0$ quantifies how the Lyapunov derivative is affected by the measurement error, with a triggering rule guaranteeing $\|e\| \leq k_0 \|x\|$ and $k_2 k_0^2 < k_1$, while $k_0 > 0$ is the design parameter in the triggering condition that restricts the size of $e(t)$ relative to $x(t)$. A full stability analysis will be included in an extended journal version.

5. SIMULATION RESULTS

In what follows, two numerical case studies are conducted to evaluate the capability and robustness of the proposed composite control framework.

5.1 Example 1

To demonstrate the controller performance, we first consider a third-order uncertain nonlinear system. The real plant is given by

$$\left\{ \begin{array}{l} \dot{z} = \underbrace{-(x_1^2 + 0.5\eta^2)z}_{f_z(x, z, \eta)}, \\ \dot{x}_1 = x_2, \\ \dot{x}_2 = \underbrace{-1.5x_1 - x_2 + 1.5(x_1 + x_2)(\sin(x_2) + 2)}_{f_0(x)}^2 \\ \quad + \underbrace{(-x_2 + \eta + z^2)}_{\Delta f(x, z, \eta)} \\ \quad + \underbrace{\left(\cos(x_1) + 2 + (\sin(x_2) - \eta)\right)u}_{g_0(x)}, \\ \quad + \underbrace{\left(\sin(x_2) - \eta\right)}_{\Delta g(x, z, \eta)}u, \\ y = x_1. \end{array} \right. \quad (6)$$

In this example, we construct the Bellman Error (BE) over a uniformly discretized exploration set \mathcal{X}_E , defined as $\mathcal{X}_E = [-2, 2]_{0.5} \times [-2, 2]_{0.5}$. The ESO parameters are selected as follows. The observer gain vector is set to $L = [2 \ 2 \ 1]^T$. The small positive constant is set to $\varepsilon = 0.03$ to accelerate ESO convergence while maintaining robustness against measurement noise.

The saturation bounds for the ESO outputs are chosen as $M_1 = M_2 = M_3 = 3$. The nominal-function saturation limits are selected as $M_f = 7, M_g = 3$, ensuring boundedness of the ESO-based control law.

Performance Analysis Fig. 2 demonstrates that the ESO performs effectively for the considered nonlinear system.

The observer-generated state trajectories closely track the actual system states, confirming the accuracy and reliability of the proposed observer.

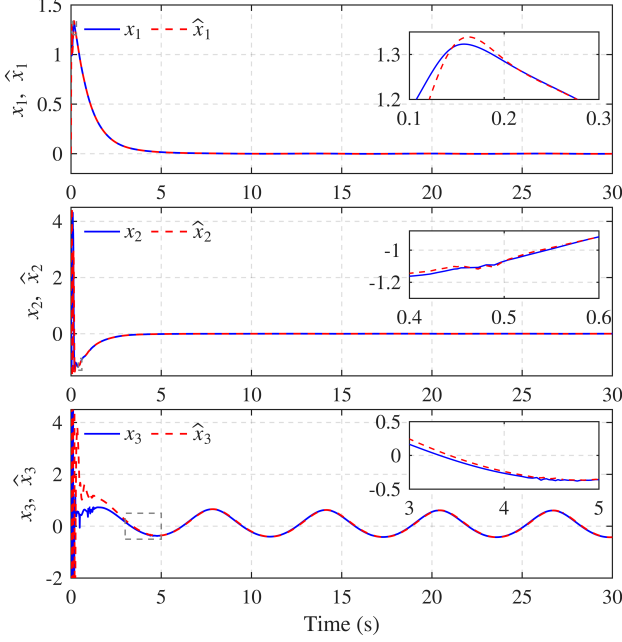


Fig. 2. System state trajectories and their ESO estimates.

Fig. 3 shows that the control input u under the proposed framework exhibits significant activity during the initial transient period due to uncertainties. After this short transient, the control input settles quickly and stays close to zero, maintaining stable behavior, indicating that the proposed control strategy achieves fast transient response and effective disturbance rejection.

To quantify the computational efficiency of the proposed ETM, we define the update saving ratio as $\eta = \frac{N_{\text{skipped}}}{N_{\text{total}}} \times 100\%$, where N_{skipped} denotes the number of skipped control updates due to the triggering condition not being satisfied and $N_{\text{total}} = N_{\text{skipped}} + N_{\text{updated}}$ represents the total number of potential update instants. Based on the simulation study, an update-saving rate of 72% is obtained, demonstrating a significant reduction in computational load while maintaining system stability.

As shown in Fig. 3, both x_1 and x_2 remain stable and converge to the equilibrium.

As illustrated in Fig. 4, the control input produced by the composite controller stays well behaved and within bounds, even when roughly 71% of its possible update instances are omitted. In contrast to the periodically updated ADP (red dashed), ETM greatly reduces the number of control updates while maintaining comparable transient response and steady-state performance.

Fig. 5 shows the distribution of triggering instants over the simulation horizon. Each cross mark represents an execution of the actor-critic update when the event-triggering condition is satisfied.

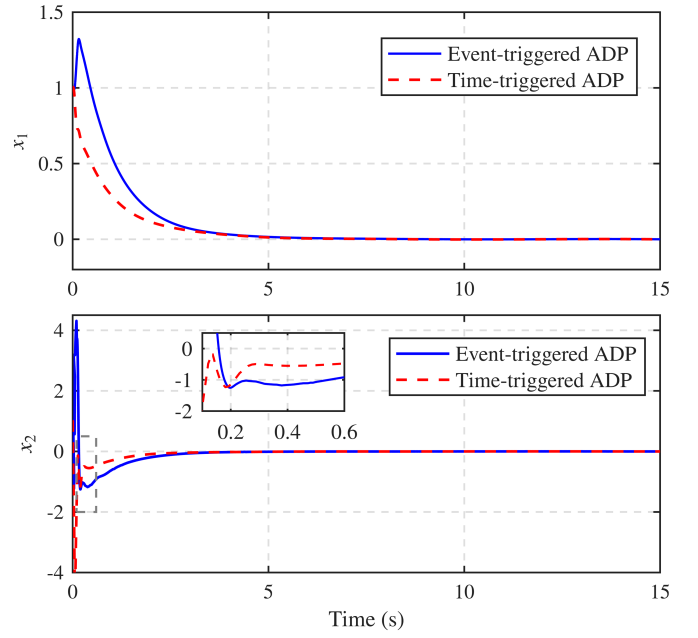


Fig. 3. State trajectories for composite control framework in Example 1

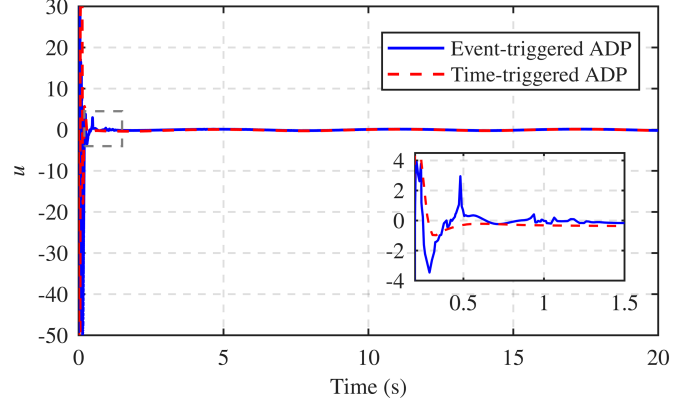


Fig. 4. Control signal composite control framework compared with those generated by the periodic ADP strategy.

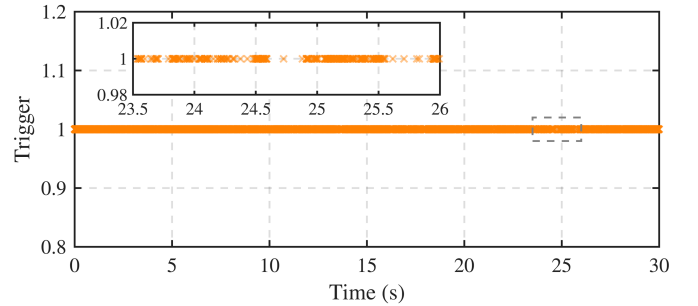


Fig. 5. Event trigger distribution

5.2 Example 2

In this example, the proposed control method is implemented on an inverted pendulum system subject to both internal and external nonlinear disturbances. The system dynamics are formulated as follows:

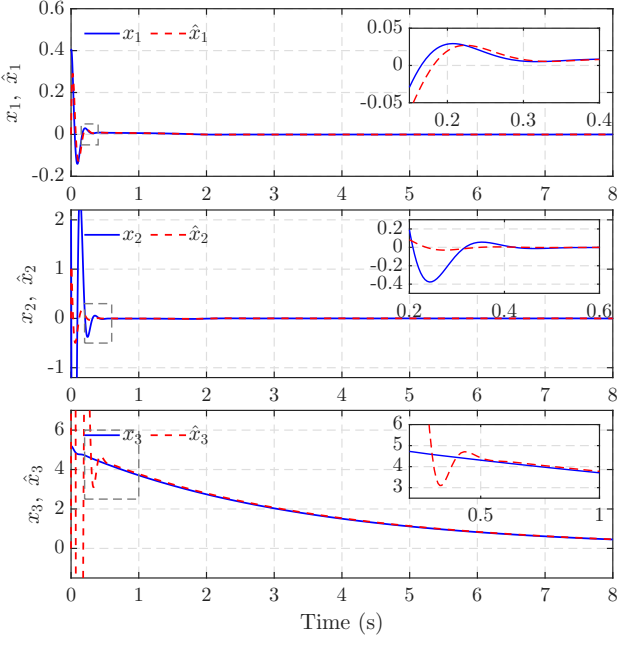


Fig. 6. System state trajectories and their ESO estimates.

$$\left\{ \begin{array}{l} \dot{z} = \underbrace{0.5 \eta(t) z}_{f_z(z, \eta)}, \\ \dot{x}_1 = \underbrace{x_2}_{f_{x_1}(x_2)}, \\ \dot{x}_2 = \underbrace{-\frac{g}{l} \sin(x_1) - \frac{b}{ml^2} x_2}_{f_0(x_1, x_2)} \\ \quad + \underbrace{5e^{-0.3t} + 0.5 \sin(x_1) + 0.5z}_{\Delta f(x_1, z, t)} + \underbrace{\frac{1}{ml^2} u}_{g_0}, \\ y = x_1. \end{array} \right. \quad (6)$$

In this example, we construct the BE over a predefined rectangular exploration set: $\mathcal{X}_E = [-2, 2]_{0.5} \times [-5, 5]_{1.0}$.

The observer gain is selected as $L = [2 \ 2 \ 1]^T$. The small positive constant used in the ESO update is set to $\varepsilon = 0.03$. The saturation bounds for the ESO states are configured as $M_1 = 1, M_2 = 1, M_3 = 3$, and the saturation bounds for the nominal functions are selected as $M_f = M_g = 7$.

The nonlinear pendulum employed in the simulation is characterized by the parameters $m = 0.8 \text{ kg}, l = 1.2 \text{ m}, b = 0.2, g = 9.81 \text{ m/s}^2$. Here m denotes the pendulum mass, l the rod length, b the viscous friction coefficient, and g is the gravitational acceleration.

Performance Analysis Fig. 6 shows that the ESO reconstructs all system states, including the aggregated disturbance term, with high accuracy. Even during fast transients and highly nonlinear phases, the estimated trajectories \hat{x}_i remain tightly aligned with the true states, showing only minimal deviation. The inset plots further demonstrate that the ESO can track fast dynamics and suppress disturbances with rapid convergence.

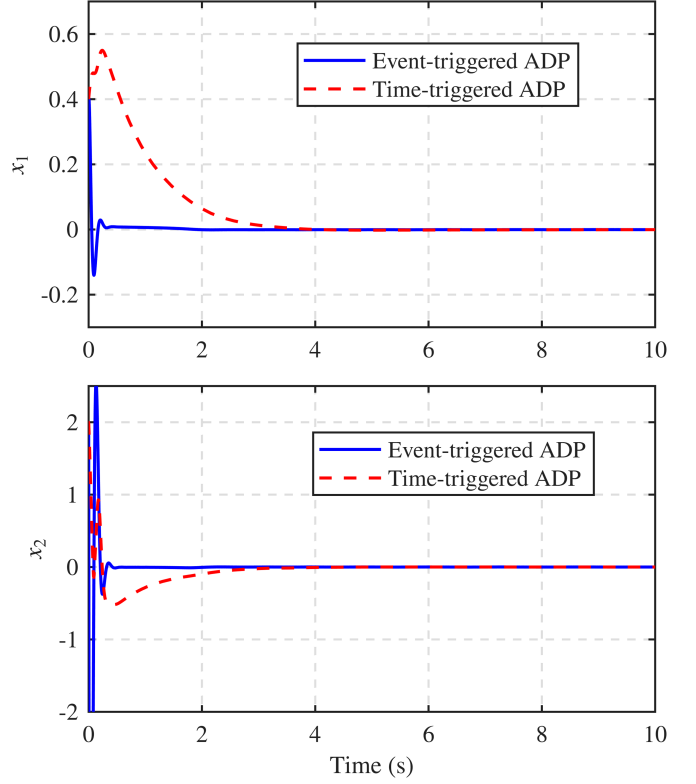


Fig. 7. Evolution of the system states from composite control framework and standard ADP method

From a theoretical perspective, Fig. 7 illustrates the main benefit of the proposed composite control framework over its time-triggered counterpart. ETM updates only when the state deviation crosses a prescribed threshold, allowing the learning and control actions to respond only to relevant changes in the dynamics. As a result, the Event Trigger (ET)-ADP achieves faster and more structured convergence, most notably in the x_2 response, which uses control and learning updates more efficiently than the uniformly sampled, time-triggered scheme. In this example, our mechanism achieved a 56% reduction in computational cost.

As depicted in Fig. 8, the proposed framework controller delivers a quick corrective action during the initial transient phase, which is expected for stabilizing the nonlinear pendulum. After the system reaches steady state, the control input rapidly decays and remains near zero, reflecting stable closed-loop behavior and low steady-state effort.

Fig. 8 further shows that the ET-ADP controller exhibits smaller amplitude variations and a faster convergence compared with the conventional time-triggered ADP. The time-triggered controller, by contrast, produces larger alternating control swings and wide input excursions, which are consistent with the overshoot and oscillatory behavior observed in Fig. 7. These results highlight the benefits of ETM: by updating only when necessary, it avoids excessive corrective actions, suppresses destabilizing oscillations, and promotes a more stable, energy-efficient control behavior.

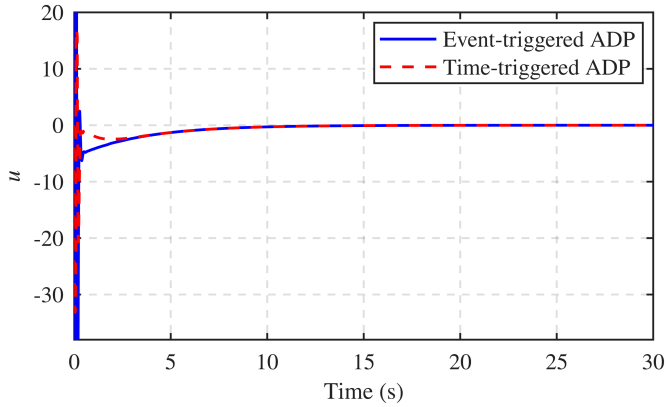


Fig. 8. Control signals generated by the proposed composite control framework, compared with those obtained from the periodic ADP strategy.

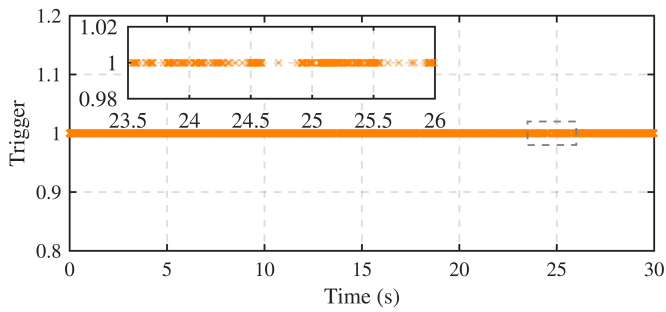


Fig. 9. Event trigger distribution

Fig. 9 depicts the timing of the triggering events during the simulation. A cross indicates an instance where the event-triggering condition prompts an actor-critic update.

6. CONCLUSION

An ESO-assisted ADP architecture with an ETM has been presented for uncertain nonlinear systems. In this framework, the ESO-based compensation scheme provides real-time estimation and removal of lumped uncertainties, while the augmented state formulation embeds the tracking error and system dynamics into the optimal control design. The ADP controller is then employed to approximate the optimal policy of the compensated subsystem through online learning. Simulation studies verify the framework's capability, showing that the controller maintains strong resistance to disturbances despite reduced update frequency enabled by the ETM. The developed methodology will be further expanded to handle multi-input-multi-output configurations in future investigations. Also, a complete hybrid-system stability proof that explicitly incorporates the triggering error will be developed in the extended journal version.

REFERENCES

Chen, W., Yang, J., Guo, L., and Li, S. (2016). Disturbance-Observer-Based Control and Related Methods—An Overview. *IEEE Transactions on Industrial Electronics*, 63(2), 1083–1095.

Dong, L., Zhong, X., Sun, C., and He, H. (2017). Event-Triggered Adaptive Dynamic Programming for Continuous-Time Systems With Control Constraints. *IEEE Transactions on Neural Networks and Learning Systems*, 28(8), 1941–1952.

Han, J. (2009). From PID to Active Disturbance Rejection Control. *IEEE Transactions on Industrial Electronics*, 56(3), 900–906.

Han, X., Zhao, X., Wang, D., and Wang, B. (2024). Event-triggered-based online integral reinforcement learning for optimal control of unknown constrained nonlinear systems. *International Journal of Control*, 97(2), 213–225.

Heemels, W., Johansson, K., and Tabuada, P. (2012). An introduction to event-triggered and self-triggered control. In *2012 IEEE 51st IEEE Conference on Decision and Control (CDC)*, 3270–3285.

Hu, J., Tang, Z., Jin, X., Zhang, B., Dong, Y., and Huang, X. (2025). Hierarchical Testing With Rabbit Optimization for Industrial Cyber-Physical Systems. *IEEE Transactions on Industrial Cyber-Physical Systems*, 3, 472–484.

Kamalapurkar, R., Walters, P., and Dixon, W. (2016). Concurrent learning-based approximate optimal regulation. *Automatica*, 64, 94–104.

Lewis, F. and Vrabie, D. (2009). Reinforcement learning and adaptive dynamic programming for feedback control. *IEEE Circuits and Systems Magazine*, 9(3), 32–50.

Lu, M., Meng, X., Huang, R., Chen, L., Tang, Z., Li, J., Peyton, A., and Yin, W. (2020). Determination of Surface Crack Orientation Based on Thin-Skin Regime Using Triple-Coil Drive-Pickup Eddy-Current Sensor.

Luo, Z., Zhang, P., Ding, X., Tang, Z., Wang, C., and Wang, J. (2020). Adaptive Affine Formation Maneuver Control of Second-Order Multi-Agent Systems with Disturbances. In *2020 16th International Conference on Control, Automation, Robotics and Vision (ICARCV)*, 1071–1076.

Onuoha, O., Kurawa, S., Tang, Z., and Dong, Y. (2024a). Discrete-Time Stress Matrix-Based Formation Control of General Linear Multi-Agent Systems.

Onuoha, O., Ubochi, B.C., Kurawa, S., Tang, Z., Wu, C., and Dong, Y. (2024b). Stress Matrix-Based Formation Control of Multi-Agent Systems with Discrete-Time Communication. In *2024 12th International Conference on Systems and Control (ICSC)*, 173–177.

Pu, Z., Yuan, R., Yi, J., and Tan, X. (2015). A Class of Adaptive Extended State Observers for Nonlinear Disturbed Systems. *IEEE Transactions on Industrial Electronics*, 62(9), 5858–5869.

Qin, X., Huang, W., Wang, X., Tang, Z., and Liu, Z. (2023). Real-Time Remaining Useful Life Prediction of Cutting Tools Using Sparse Augmented Lagrangian Analysis and Gaussian Process Regression. *Sensors*, 23(1), 413.

Ran, M., Li, J., and Xie, L. (2021). A new extended state observer for uncertain nonlinear systems. *Automatica*, 131, 109772.

Ran, M., Li, J., and Xie, L. (2022). Reinforcement-Learning-Based Disturbance Rejection Control for Uncertain Nonlinear Systems. *IEEE Transactions on Cybernetics*, 52(9), 9621–9633.

Tabuada, P. (2007). Event-Triggered Real-Time Scheduling of Stabilizing Control Tasks. *IEEE Transactions on Automatic Control*, 52(9), 1680–1685.

Tang, Z. (2019). *Control design for the active magnetic bearing system*. The University of Manchester (United Kingdom).

Tang, Z., Chen, X., Jin, X., Zhang, B., and Liang, W. (2025). A temporal scale transformer framework for precise remaining useful life prediction in fuel cells.

Tang, Z., Passmore, C., Rossiter, A., Ebbens, S., Dunderdale, G., and Panoutsos, G. (2024a). Disturbance Observer-Based Optimal Tracking Control for Slot Coating Process with Mismatched Input Disturbances. In *2024 UKACC 14th International Conference on Control (CONTROL)*, 55–56.

Tang, Z., Rossiter, A., Dong, Y., and Panoutsos, G. (2024b). Reinforcement Learning-Based Output Stabilization Control for Nonlinear Systems With Generalized Disturbances. In *2024 IEEE International Conference on Industrial Technology (ICIT)*, 1–6.

Tang, Z., Rossiter, A., Jin, X., Zhang, B., and Panoutsos, G. (2024c). Output Tracking for Uncertain Time-Delay Systems via Robust Reinforcement Learning Control. In *2024 43rd Chinese Control Conference (CCC)*, 2219–2226.

Tang, Z., Rossiter, A., and Panoutsos, G. (2024d). A Reinforcement Learning-Based Approach for Optimal Output Tracking in Uncertain Nonlinear Systems with Mismatched Disturbances. In *2024 UKACC 14th International Conference on Control (CONTROL)*, 169–174.

Tang, Z., Wang, C., and Ding, Z. (2016). Unmatched disturbance rejection for AMB systems via DOBC approach. In *2016 35th Chinese Control Conference (CCC)*, 5931–5935.

Tang, Z., Yu, Y., Li, Z., and Ding, Z. (2019). Disturbance rejection via iterative learning control with a disturbance observer for active magnetic bearing systems. *Frontiers of Information Technology & Electronic Engineering*, 20(1), 131–140.

Xue, S., Luo, B., Liu, D., and Li, Y. (2020). Adaptive dynamic programming based event-triggered control for unknown continuous-time nonlinear systems with input constraints. *Neurocomputing*, 396, 191–200.

Yao, Y., Tang, Z., and Zeng, L. (2025). From learning to adoption: Understanding marketing students' acceptance of generative ai technologies. In *2025 Global Marketing Conference at Hong Kong Proceedings*.

Zhang, B., Jin, X., Liang, W., Chen, X., Li, Z., Panoutsos, G., Liu, Z., and Tang, Z. (2024). TabNet: Locally Interpretable Estimation and Prediction for Advanced Proton Exchange Membrane Fuel Cell Health Management. *Electronics*, 13(7), 1358.

Zhao, H., Tang, Z., Li, Z., Dong, Y., Si, Y., Lu, M., and Panoutsos, G. (2024). Real-Time Object Detection and Robotic Manipulation for Agriculture Using a YOLO-Based Learning Approach. In *2024 IEEE International Conference on Industrial Technology (ICIT)*, 1–6.